Liquid-Liquid Phase Separation in Hemoglobins: Distinct Aggregation Mechanisms of the β6 Mutants

Qiuying Chen,* Peter G. Vekilov,† Ronald L. Nagel,*‡ and Rhoda Elison Hirsch*§
*Department of Medicine, Division of Hematology, Albert Einstein College of Medicine, Bronx, New York; †Department of Chemical Engineering, University of Houston, Houston, Texas; ‡Department of Physiology and Biophysics, and §Department of Anatomy and Structural Biology, Albert Einstein College of Medicine, Bronx, New York

ABSTRACT Reversible liquid-liquid (L-L) phase separation in the form of high concentration hemoglobin (Hb) solution droplets is favored in an equilibrium with a low-concentration Hb solution when induced by inositol-hexaphosphate in the presence of polyethylene glycol 4000 at pH 6.35 HEPES (50 mM). The L-L phase separation of Hb serves as a model to elucidate intermolecular interactions that may give rise to accelerated nucleation kinetics of liganded HbC (β6 Lys) compared to HbS (β6 Val) and HbA (β6 Glu). Under conditions of low pH (pH 6.35) in the presence of inositol-hexaphosphate, COHb assumes an altered R-state. The phase lines for the three Hb variants in concentration and temperature coordinates indicate that liganded HbC exhibits a stronger net intermolecular attraction with a longer range than liganded HbS and HbA. Over time, L-L phase separation gives rise to amorphous aggregation and subsequent formation of crystals of different kinetics and habits, unique to the individual Hb. The composite of R- and T-like solution aggregation behavior indicates that this is a conformationally driven event. These results indicate that specific contact sites, thermodynamics, and kinetics all play a role in L-L phase separation and differ for the β6 mutant hemoglobins compared to HbA. In addition, the dense liquid droplet interface or aggregate interface noticeably participates in crystal nucleation.

INTRODUCTION

Protein-protein attractive interaction, resulting in the formation of protein solid phases, underlies the mechanistic basis of a variety of condensation diseases that includes, for example, sickle cell anemia (for a review, see Eaton and Hofrichter, 1990), homozygous CC disease caused by crystal formation in erythrocytes of humans expressing β^C hemoglobin (for a review, see Nagel and Lawrence, 1999; Nagel and Steinberg, 2001), the eye cataract (Benedek et al., 1999; Annunziata et al., 2003), Alzheimer's disease, and Huntington's disease (Dumery et al., 2001; Chuang et al., 2002; Crowther, 2002). In vitro studies of aggregating proteins, particular to the sickle hemoglobin polymer or the eye cataract, demonstrate the occurrence of the liquid-liquid (L-L) phase separation (i.e., formation of a dense liquid phase) that precedes polymerization or crystallization (Galkin et al., 2002; Benedek et al., 1999; Annunziata et al., 2003). This protein high concentration liquid phase is metastable with respect to the solid and can mediate transition to the ordered aggregate (Hagen and Frenkel, 1994; ten Wolde and Frenkel, 1997). L-L phase separation also serves as a direct tool for probing protein-protein interactions (Annunziata et al., 2002, 2003).

In vitro L-L phase separation of hemoglobin has been observed by different laboratories lending insight into sickle cell hemoglobin (HbS) intermolecular interactions (San Biagio and Palma, 1991; Serrano et al., 2001; Galkin et al., 2002; Vaiana et al., 2003). Direct evidence demonstrated that L-L phase separation occurs in vitro in human hemoglobin at or near physiological pH after the addition of small amount of additives such as 0.25–1.0% (w/v) polyethylene glycol (PEG) 8000 (Galkin et al., 2002). L-L phase separation of high concentrations of both liganded R-(oxy)state and T-(deoxy)state HbA (β6 Glu) and HbS (β6 Val) occurs at similar temperature at neutral pH (Galkin et al., 2002). However, only the dense liquid droplets in deoxy HbS facilitate the nucleation of polymers. The L-L separation boundary shifts with the addition of nontoxic additives such as PEG at molar concentrations 30 times lower than Hb. Thus, utilization of the L-L separation phase boundary of deoxy HbS opens avenues that may control strategies to inhibit HbS polymerization (Galkin and Vekilov, 2000; Galkin et al., 2002). These in vitro findings highlight the value of L-L phase separation as a probe of mechanisms underlying the ligand-dependent self-aggregating β6 hemoglobin (Hb) variants: in red blood cells and in vitro, sickle Hb (HbS) that polymerizes in the deoxy (T-state) (Eaton and Hofrichter, 1990), and HbC (β6 Glu→Lys) that crystallizes in the oxy form (R-state) (Hirsch et al., 1985; Lawrence et al., 1991; Nagel and Lawrence, 1999; Nagel and Steinberg, 2001).

In the present study, L-L phase separation is used as a model to elucidate intermolecular Hb-Hb interactions and mechanisms involved in the enhanced nucleation kinetics/crystallization of liganded HbC compared to HbA and HbS. The in vitro conditions used here to affect a predominating L-L phase separation of R-state hemoglobins allows for the amplification, and thus analysis, of differences in molecular interactions among these hemoglobins. We report here that

Submitted April 21, 2003, and accepted for publication October 23, 2003.

Address reprint requests to Dr. Rhoda Elison Hirsch, Dept. of Medicine and Dept. of Anatomy and Structural Biology, 1300 Morris Park Ave., Bronx, NY 10461. Tel.: 718-430-3604; Fax: 718-824-3153; E-mail: rhirsch@aecom.yu.edu.

0006-3495/04/03/1702/11 $2.00

reversible L-L phase separation shows significant differences between mutant hemoglobins (HbC and HbS) and HbA at low pH (pH 6.35) in the presence of the allosteric effector inositol-hexaphosphate (IHP) and polymer PEG. The relevance of this L-L phase separation model, under the conditions investigated, is further indicated by the formation of crystals and fibers arising from the metastable L-L phase separation of the respective liganded $\beta 6$ mutant, which is not observed for HbA under the same conditions. In addition, it is found that the dense liquid droplet interface and aggregate interface play a significant role in crystal nucleation.

MATERIALS AND METHODS

Materials

PEG was obtained from Sigma-Aldrich (St. Louis, MO) and used without further purification. A 50% (w/v) stock solution of PEG 4000 was prepared in 50 mM HEPES buffer. The pH of this PEG solution was carefully adjusted to the desired pH by HEPES salt or HEPES acid. Dextran was also obtained from Sigma-Aldrich.

Hb was purified as described earlier (Hirsch et al., 1999). Stripped COHb at pH 7.35 was dialyzed against pH 6.35 50 mM HEPES buffer and was used throughout the study. A sodium salt of IHP was obtained from Sigma. A 200 mM IHP stock solution was passed through an Amberlite column (Rohm and Haas, Philadelphia, PA) and recycled as described previously (Amiconi and Giardina, 1981). A stock solution of IHP (10 mM) was prepared in 50 mM HEPES at pH 6.35.

Solution conditions and batch methods for generating L-L phase separation

In a small PCR tube, buffer of 50 mM HEPES at pH 6.35 and PEG were mixed well by vortexing for 5 s; then COHb and IHP were added and gently mixed. Phase separation occurs directly after addition of IHP. As shown below, this phase separation is reversible upon changing temperature. In addition to L-L phase separation, the subsequent growth of crystals and the formation of a macroscopically amorphous solid phase aggregate were observed when higher PEG and IHP concentrations ($\sim$1.0 g/dl COHb, 10% PEG, and 4:1 IHP:Hb) were used.

Measurement of T_{cloud}, $T_{clarify}$, and the L-L phase boundary $T_{L\text{-}L}$

Measurement of phase separation temperature is carried out with the use of a programmable PCR instrument (temperature variability $\pm$ 0.2°C) (HYBAID PCR Express, Thermo Electron, Middlesex, UK). The turbid (cloudy) solution was incubated for 10 min starting at 4°C with increments of 5°C and ending at 45°C. The temperature at which the solution becomes clear was recorded. Then, the temperature was decreased by 2°C steps until the solution becomes cloudy. T_{cloud} is the temperature for the onset of the phase separation, at which no change in turbidity occurs when the temperature is further decreased by 2°C steps. After the determination of T_{cloud}, the temperature is raised in 2°C steps and $T_{clarify}$ is recorded as the temperature at which the cloudy solution becomes clear, according to the method of Broide et al. (1991). The liquid-liquid phase separation temperature ($T_{L\text{-}L}$) was obtained as the mean of $T_{clarify}$ and T_{cloud}. It should be mentioned that the determination of $T_{L\text{-}L}$ described above was performed in solutions where no crystals or amorphous phase were observed when viewed microscopically. In the protein solution, the dense liquid phase is metastable (Hagen and Frenkel, 1994; ten Wolde and Frenkel, 1997) and over time decays into a solid phase: crystals, polymers, and/or aggregates. However, with the hemoglobin variants studied here, the formation of the respective solid phase is slow and the dense liquid droplets are preserved under the conditions used for $T_{L\text{-}L}$ measurements, such that L-L separation can be reversed and reestablished repeatedly without hysteresis (Galkin and Vekilov, 2000).

Refractive index measurements

A Bauch and Lomb refractometer (Rochester, NY) was used to measure the refractive index of PEG in the supernatant of the L-L phase separation mixture after centrifugation. The PEG concentration was determined from the standard calibration curve of PEG (linear regression of PEG concentration versus PEG refractive index).

Microscopy

An Axiovert 405M microscope (Zeiss, Oberkochen, Germany) with and without video enhancement, and with capabilities of differential interference contrast (DIC) imaging, was used to observe phase separation, amorphous aggregation, and crystal growth. (This microscope setup is described in detail in Hirsch et al., 2001.) The black and white images, shown in the figures, are DIC video-enhanced (4000× magnification), whereas the color images are derived from standard oil-immersion light microscopy optics (1000× magnification).

RESULTS

L-L phase separation in COHbA, C, and S in the presence of IHP and PEG at pH 6.35

The hemoglobins, under the conditions used in this study, exhibit L-L phase separation that typically appears as liquid droplets of a high protein density suspended in the Hb mother solution. (A description of classic protein L-L phase separation is found in McPherson et al., 2000.) A mixture of COHb (0.5–10 g/dl), PEG 4000 (2–10%), and IHP (1:1–4:1 IHP:Hb) result in classical reversible L-L phase separation occurring in the form of droplets that appear identical to that observed for deoxy HbS (Serrano et al., 2001; Galkin et al., 2002) (Fig. 1). A working pH of 6.35 was selected since COHb at this pH forms an altered R-state conformation that binds IHP (Scott et al., 1983). CO also provides enhanced stability compared to the oxy-liganded form of hemoglobin. At the concentration of R-state Hb employed in these solutions containing IHP and PEG, the tetramer predominates and dissociation to dimers is insignificant (Herskovits et al., 1977; Antonini and Brunori, 1971).

To dissect out the mechanistic basis for the high propensity of liganded HbC to crystallize, a comparison to normal Hb (HbA) and the other $\beta 6$ self-aggregating Hb (HbS) is warranted. Under the same experimental conditions and specific to the Hb variant, the droplets vary in amount and dimension (Fig. 1). A concentration distribution of Hb in the droplets is apparent under light microscopy. The droplets can be separated by centrifugation or settle to the bottom upon standing. HbC exhibits smaller droplets (diameter < 5 μm) and in greater total number than HbS and HbA (Fig. 1).

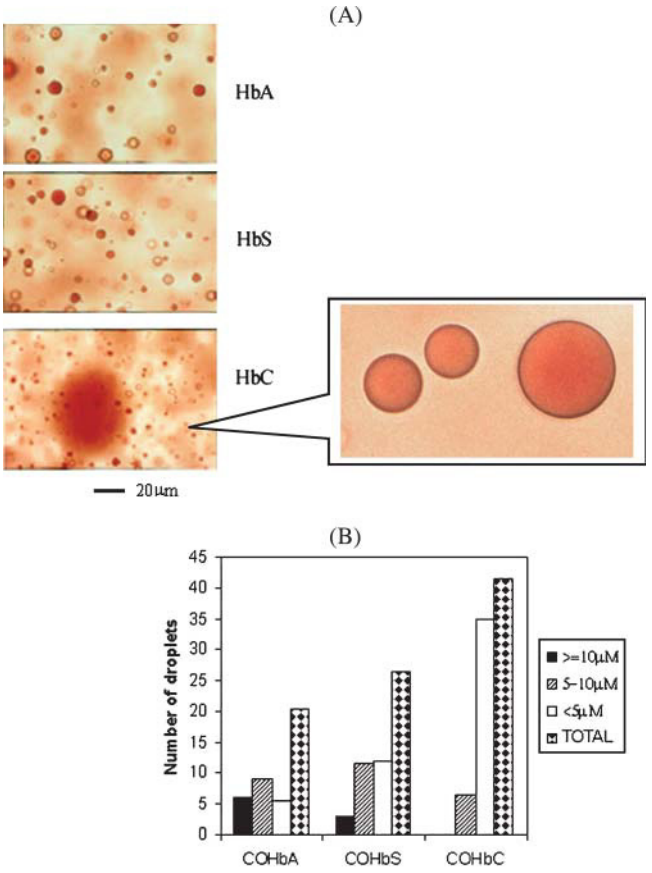

FIGURE 1 Formation of (*A*) COHbA, C, and S droplets and (*B*) droplet counts in the presence of IHP and PEG 4000 (50 mM HEPES at pH 6.35). The initial solution contained 1.0 g/dl COHb, 2:1 IHP:Hb, and 10% PEG 4000, 4°C. Bar = 20 μm.

Dextran (MW 67,300), a polysaccharide, and anions such as chloride and nitrate, serve as controls to determine the efficiency and specificity of PEG and IHP, respectively, in inducing L-L separation. The hemoglobin phase separation properties are significantly different in the presence of dextran. A dextran concentration up to 10% did not induce L-L phase separation. However, at higher concentrations of dextran (>18%), minimal L-L phase separation occurred, with most of the Hb remaining in solution. In the absence of IHP but in the presence of PEG, chloride or nitrate does not induce L-L phase separation.

The equilibrium between the phases of a multicomponent system is depicted by a phase diagram [binodal (coexistence curve)]

The position of the L-L phase boundaries provides insight about the nature and magnitude of the protein-protein interaction (Lomakin et al., 1996; Muschol and Bonnete, 1996; Grigsby et al., 2001). The phase diagram of a multicomponent system represents the conditions of equilibrium between the phases. A schematic phase diagram of a two-component system undergoing liquid-liquid phase separation in the (*Concentration, Temperature*) plane is shown in Fig. 2. The solid line represents the conditions under which the high- and the low-density phases are in equilibrium. Thus, for each temperature T, we can find the concentrations of each of the two phases in equilibrium. A homogeneous solution is stable at the concentration and temperature that corresponds to a point above this so-called L-L coexistence or binodal line. If a homogeneous solution is cooled to (*Concentration, Temperature*) below the L-L binodal, it undergoes separation into a low and a high-density phase with compositions indicated on the binodal at this T. At temperatures just slightly below $T_{L\text{-}L}$ (i.e., low undercoolings), the generation of new droplets has to overcome a thermodynamic barrier, i.e., the droplets are generated by nucleation. This is the region of metastability of the undercooled homogeneous solution. At high undercoolings, this barrier vanishes, the undercooled homogenous solution is unstable, and the process of generation of new phases is referred to as spinodal decomposition (Cahn and Hilliard, 1958; Puri and Binder, 2001). The boundary between the regions of metastability and instability is called the spinodal line.

In the Discussion, we only address phase separation at low undercoolings occurring via nucleation. At a certain temperature, the concentrations of the two phases in equilibrium coincide, and the binodal touches the spinodal. This is referred to as the critical point (C^{crit}, T^{crit}). The binodal curves for L-L phase separation of COHbA, COHbC, and COHbS solutions containing 5% PEG 4000, 4:1 IHP:Hb, and 50 mM HEPES at pH 6.35 are shown in Fig. 3. In these plots, the solution was viewed as consisting of two components: the respective Hb and the solvent.

The experimental points were fitted to the equation of Stanley (1971), as modified by Muschol and Rosenberger (1997),

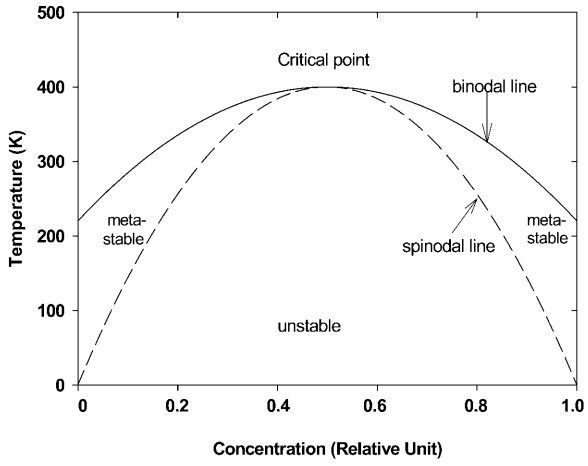

FIGURE 2 A classical concentration-temperature phase diagram. Modified from www.poco.phy.cam.ac.uk/teaching/A_Donald/Phase_Diagrams.pdf.

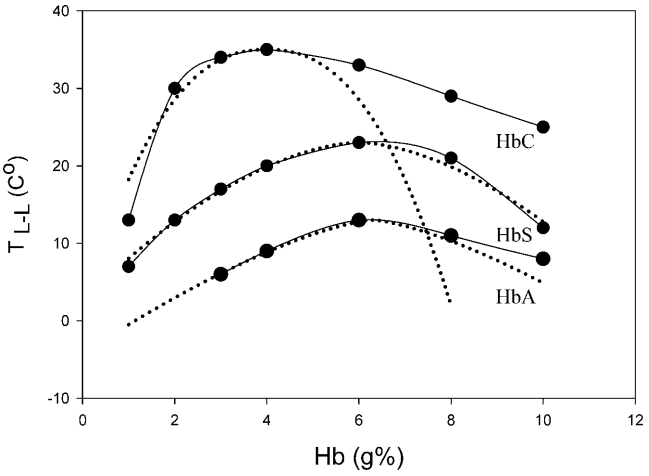

FIGURE 3 Binodal curves of COHbA, C, and S experimentally measured (*solid line*) and plotted from Eq. 1 (*dashed line*). (5% PEG 4000, 4:1 IHP:Hb, and 50 mM HEPES at pH 6.35.)

$$T_{\text{L-L}} = T^{\text{crit}}\{1 - A|(C^{\text{crit}} - C)/C^{\text{crit}}|^{1/\beta}\}, \qquad (1)$$

where T^{crit} and C^{crit} are critical temperature and concentration, respectively. β is the critical exponent (Vega et al., 1992) and A is an amplitude. β and A are dimensionless. Liganded HbA and HbS have symmetric binodal curves, which overlap with those generated from the above equation. Liganded HbC exhibits a rather unusual asymmetric curve. This observation implies unique intermolecular interactions for HbC that are discussed below.

A comparison of the critical parameters for liganded HbA, C, and S is shown in Table 1. It is noteworthy that the binodal curves of the three COHbs differ with respect to T^{crit} and C^{crit}. COHbC has a higher $T_{\text{L-L}}$ than HbS and HbA under the same experimental conditions. A higher T^{crit} is an indication of stronger net attractive interaction between proteins (Grigsby et al., 2001), which will be discussed further in this article.

Modulation of binodal curves by the solution components

In vivo, hemoglobin function is regulated by allosteric effectors such as 2,3-diphosphoglycerate (DPG) and chloride (for one of many reviews, see Imai, 1982). IHP, an analog of DPG, has often been used to probe Hb structure and function. Since the characteristics of the phase diagram provide insight into intermolecular interaction between protein molecules (Lomakin et al., 1996; Muschol and Bonnete, 1996; Grigsby et al., 2001), modulation of the phase diagram (binodal curve) by solution components such as IHP, chloride, and nontoxic additives such as PEG is of interest.

The propensity for L-L phase separation of COHbA, C, and S increases with higher concentration of IHP and PEG. Measurement of the refraction index of the supernatant demonstrates that PEG was excluded from the Hb dense phase (Table 2). The percent of Hb recruited into the phase separation, analyzed by centrifugation and Hb concentration, increases with an increase in IHP:Hb ratio and PEG concentration (data not shown).

The concentration of IHP and PEG also affects binodal curves of the L-L phase separation of COHbA, C, and S (Fig. 4). At decreasing IHP or PEG concentration, phase separation of CO-liganded hemoglobins occurs at a lower $T_{\text{L-L}}$ and requires higher Hb concentration (Fig. 4). Specifically, due to the formation of needle crystals and other amorphous aggregates during the time of measurement (10 min), $T_{\text{L-L}}$ of COHbS is not attainable under the following conditions investigated: 10% PEG, 4:1 IHP, and 1.0–10.0 g/dl COHbS; and 10% PEG, 2:1 IHP, and COHbS $>$ 6.0 g/dl (Fig. 4 *C*).

Similar to COHbS, the $T_{\text{L-L}}$ for COHbC at concentrations $>$2.0 g/dl (in the presence of 10% PEG and 4:1 IHP:Hb) is not attainable due to the formation of aggregates and crystals (Fig. 4 *A*). However, with the addition of salts such as sodium chloride, $T_{\text{L-L}}$ is measurable for COHbC over the concentration range (1.0–10 g/dl) (Fig. 5 *A*). In direct contrast, even in the presence of up to 0.1 M chloride, $T_{\text{L-L}}$ for COHbS was not attainable as mentioned above. It is noteworthy that for COHbA and COHbC, the addition of chloride results in a lower $T_{\text{L-L}}$ with phase separation occurring at higher COHbC and COHbA concentration (Fig. 5, *A* and *B*).

In vitro COHb L-L phase separation subsequently gives rise to amorphous aggregation and crystal growth

Although L-L phase separation may mediate the transition to nucleation and crystal growth, it is not a prerequisite

TABLE 1 A comparison of the critical parameters for HbA, C, and S

COHb	T^{crit} (°C)	C^{crit} (g/dl)	ϕ^{crit}	β	A
COHbA	13	6.3	0.04977	0.708	1.3251
COHbC	35	4.0	0.0316	0.4253	0.9428
COHbS	23	6.0	0.0474	0.5859	0.888

Conditions: 5% PEG 4000, 4:1 IHP:Hb, and 50 mM HEPES, at pH 6.35.

TABLE 2 PEG concentrations in the supernatant of the L-L phase separation solution

COHbC (g/dl)	PEG added (w/v%)	IHP:Hb	Refraction index	PEG in supernatant (w/v%)
1.0	10	4:1	1.3545	10.5
2.0	10	4:1	1.3540	10.2

Conditions: 50 mM HEPES, at pH 6.35.

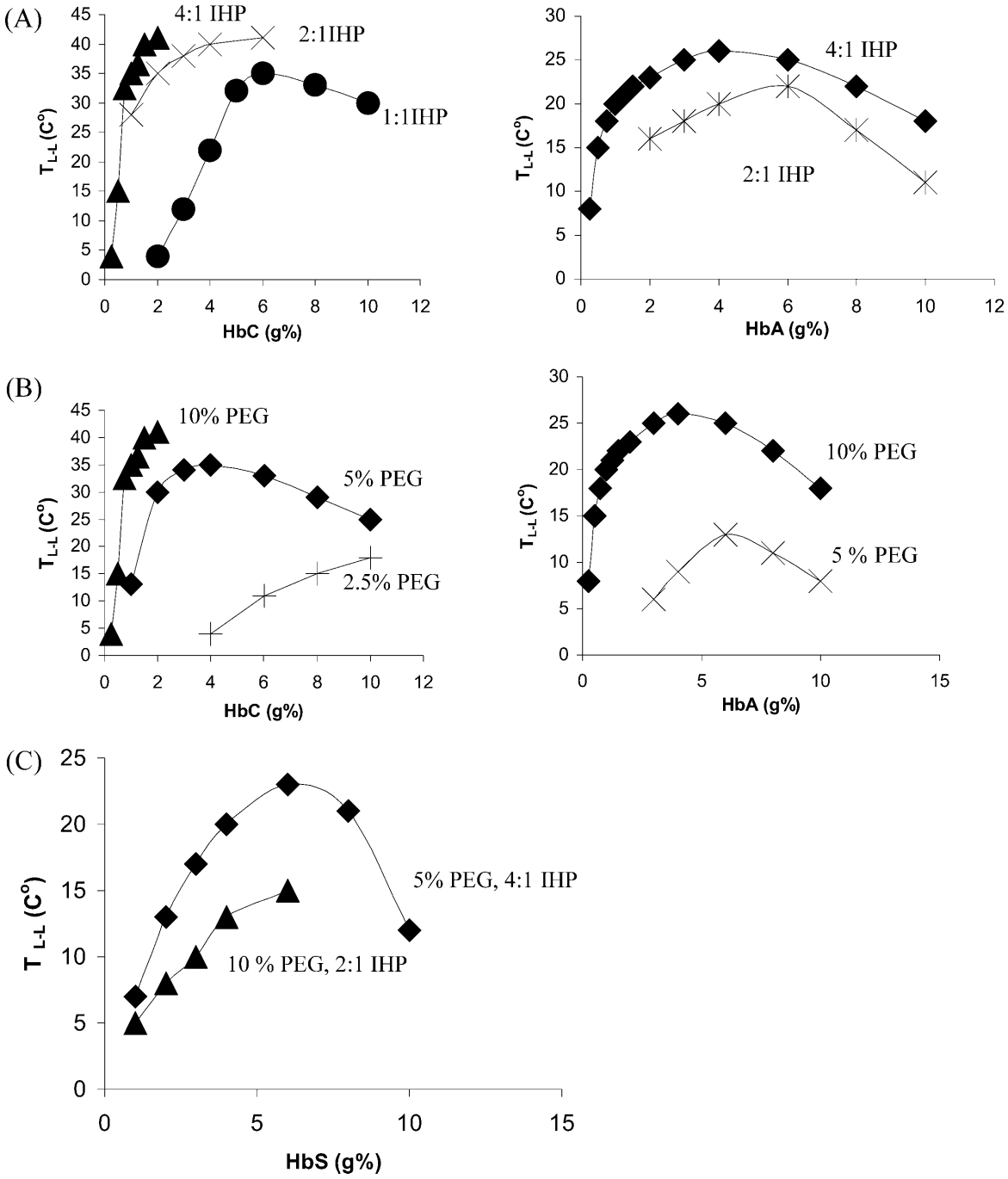

FIGURE 4 IHP and PEG modulation of binodal curves of L-L phase separations: COHbA, COHbC, and COHbS (50 mM HEPES at pH 6.35). (*A*) The IHP effect on COHbC and COHbA at 10% PEG, $T_{L\text{-}L}$ for COHbC >2.0 g/dl, is not attainable due to the formation of aggregates and crystals during measurement (see text). (*B*) The PEG effect on COHbC and COHbA at 4:1 IHP:COHb. (*C*) IHP and PEG significantly affect the binodal curve of COHbS. Under certain conditions (e.g., *A* and *B*), $T_{L\text{-}L}$ for COHbS is not attainable due to the formation of crystals and aggregates within the time of measurement (see text).

(McPherson, 1985; Ray and Bracer, 1986; Kuznetsov et al., 1999, 2001). Nevertheless, since L-L phase separation is used in this study as a means to amplify and define mechanisms of enhanced liganded HbC nucleation and crystallization, it is then important to demonstrate for the conditions employed that the observed hemoglobin L-L phase separation mediates transition to crystal growth. Under the given experimental conditions (1.0 g/dl Hb, 10% PEG, and 4:1 IHP:Hb at pH 6.35), differential aggregation behaviors are observed after the respective L-L phase separation for the $\beta 6$ mutant hemoglobins and HbA. COHbC forms tetragonal, hexagonal, and orthorhombic crystals

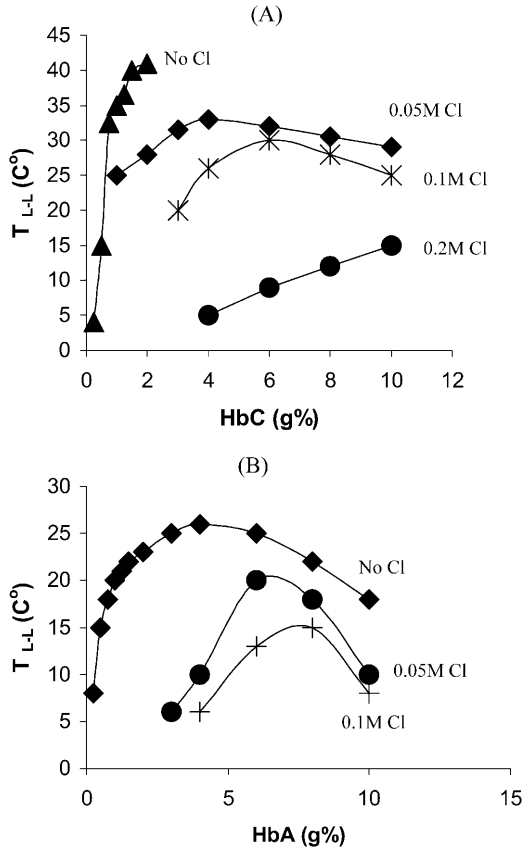

FIGURE 5 Chloride significantly affects the binodal curves of (*A*) COHbC and (*B*) COHbA (10% PEG, 4:1 IHP:Hb, and 50 mM HEPES at pH 6.35). Note that because COHbS (1.0–10.0 g/dl) forms needle crystals even in the presence of up to 0.1 M chloride, the chloride effect on the COHbS binodal curve is not attainable (see text).

within 5 h (Fig. 6). It is noteworthy that when dextran is substituted for PEG in the initial solution, COHbC nucleation and crystal growth did not occur for up to at least three days.

Light and DIC microscopies show that some precrystalline aggregates of HbC form inside of the dense Hb protein droplets (Fig. 6 *A*). However, most crystals grow from the edge of the droplets or aggregates (Fig. 6, *B* and *C*). Crystals of different habits may grow at the interface of a single droplet or aggregate (Fig. 6, *B* and *C*, *left images*), whereas others may form one class of crystal habit (Fig. 6 *C*, *middle* and *right images*). Some droplets within the same time frame give rise to single hexagonal and orthorhombic crystals (Fig. 6 *D*, *middle* and *right images*).

COHbS forms spherulite domains within 2 min (Fig. 7 *A*); needle-like crystals (Fig. 7 *B*), fascicles of macrofibers (Fig. 7 *C*, *left* and *middle image*), and radiant macrofibers (Fig. 7 *C*, *right image*) form within 10 min, whereas COHbA maintains its L-L phase separation in droplet form up to at least 24 h of incubation. However, at higher COHbA concentration (COHbA $>$ 3.0 g/dl), long orthorhombic crystals formed after 22 h of incubation (Fig. 8).

DISCUSSION

Conformational alterations and intermolecular interactions are reflected in comparative liquid-liquid phase separation

Liganded Hb L-L phase separation requires the participation of both IHP and PEG at pH 6.35. IHP is known to bind COHb at pH 6.35, resulting in an altered R-state conformation (Scott et al., 1983). Interestingly, the recently reported high-resolution structure of COHbA, derived from crystals grown at pH 6.4 in concentrated phosphate buffer, shows R-state tertiary changes (Safo et al., 2002). In addition to a significant movement and weakening of two hydrogen bonds involving $\alpha 1\beta 2$ interface residues (critical for the definition of R-state), a phosphate molecule is bound at the β-subunit terminus of the central cavity, at the exact position occupied by DPG in T-state Hb (Safo et al., 2002). This latter observation provides strong evidence that 1) IHP, DPG, or DPG analogs bind to the DPG pocket in liganded Hb under conditions of low pH as previously demonstrated by quantitative biophysical and biochemical techniques (Scott et al., 1983; Gottfried et al., 1997; Hirsch et al., 1996, 1999); and 2) substantiates the use of IHP, under conditions of pH 6.35, to probe site-specific conformational differences in the $\beta 6$ Hb variants (Hirsch et al., 1996, 1997, 1999).

Although crystallographic studies indicate that hemoglobins A, C, and S have similar quaternary crystal structures, solution studies using spectroscopic (front-face fluorescence and ultraviolet resonance Raman) probing point to conformational differences distal to the site of the $\beta 6$ mutation (Hirsch et al., 1996, 1997, 1999). IHP amplifies the conformational difference between HbA and the $\beta 6$ mutants (Hirsch et al., 1999). This is also reflected in the distinct solution L-L phase separation behaviors of HbA, C, and S shown in this study. However, Galkin et al. (2002) showed that both oxy and deoxy HbA and HbS have similar L-L phase separation temperature (35–40°C) at or near physiological pH, ionic strength, and Hb concentration (0.15 M pH 7.35 phosphate buffer, 0.1–1.0% w/v PEG 8000, 9.6–19 g/dl Hb). The apparent discrepancy is likely due to the different experimental conditions: pH, ionic strength, and the presence of IHP. The low ionic strength environment (in 50 mM HEPES buffer) of this study provides advantages for the most pronounced pH-dependent changes in intermolecular forces: at low ionic strengths, the Coulomb and the other electrostatic interactions (dipole, etc.) are only weakly screened and provide a significant contribution to the intermolecular interaction potential.

PEG is another vital component for the observed L-L phase separation. PEG, a benign nonionic water-soluble polymer, is often used to induce L-L phase separation in proteins. Several studies have focused on the effect of PEG on protein intermolecular interactions using small-angle x-ray scattering (Tardieu et al., 1999; Finet and Tardieu, 2001; Tanaka and Ataka, 2002; Annunziata et al., 2002). It was shown that PEG

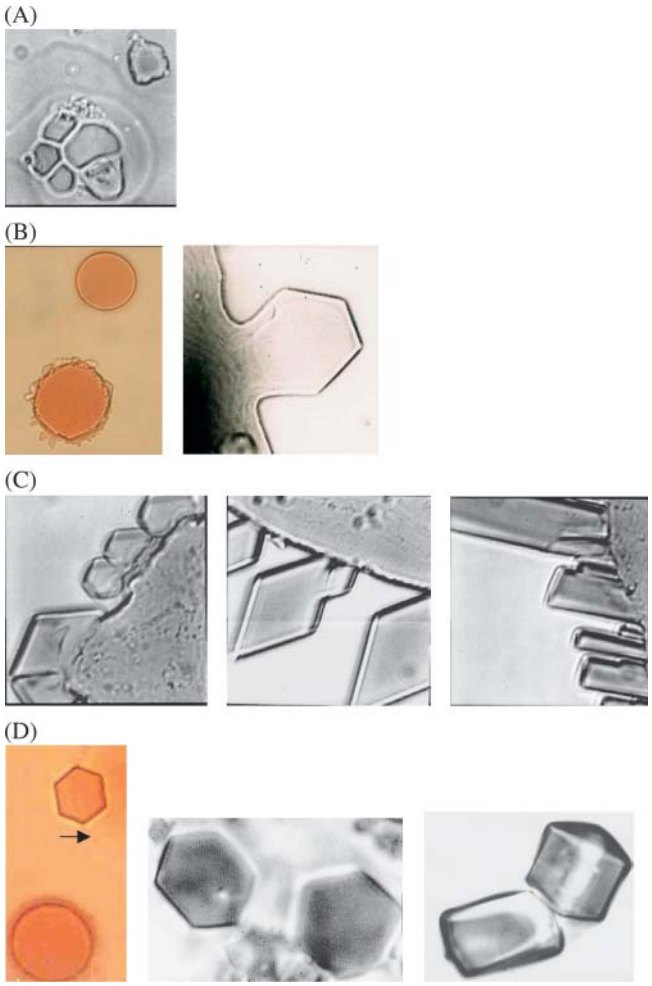

FIGURE 6 Hemoglobin C crystals and aggregates after L-L phase separation. Crystals notably grow at the liquid droplet or aggregate interface edge (50 mM HEPES at pH 6.35, 1.0 g/dl COHbC, 4:1 IHP:Hb, and 10% PEG 4000, 20°C). (*A*) Less commonly, precrystalline structures of HbC form inside of liquid droplets by ~2 h. (*B*, *left image*) A liquid droplet, and a denser liquid droplet with both tetragonal and orthorhombic crystals growing at the interface (~2.5 to >5 h). (*B*, *right image*) A hexagonal crystal in the process of forming at the interface of a liquid droplet. (*C*) Crystals growing from the edge of aggregates by ~5 h; crystals of different habits grow at the surface of a single aggregate (*C*, *left image*), or from different aggregates (*C*, *middle* and *left images*). (*D*) Hexagonal and tetragonal crystals form at ~5 h. (*D*, *left image*) A liquid droplet, and a liquid droplet giving rise to a hexagonal crystal—the arrow points to the liquid droplet surface from which hemoglobin molecules appear to be recruited. (*D*, *middle image*) Hexagonal crystals formed from liquid droplets. (*D*, *right image*) Orthorhombic crystals formed from liquid droplets. It is known that crystals of different habits form under the same condition (e.g., McPherson, 1982) or within a single liquid droplet (Durbin and Feher, 1996). Color, at 1000× magnification; black and white, at 4000× magnification. (See Materials and Methods for explanation.)

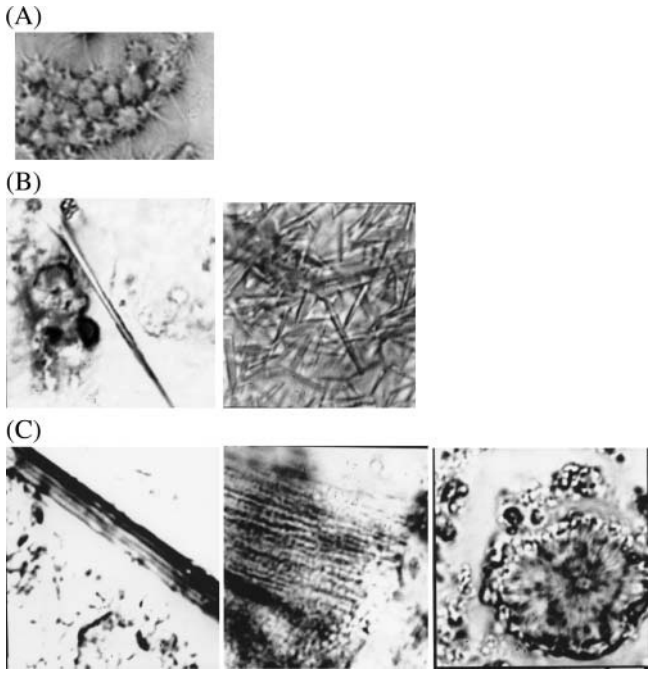

FIGURE 7 The formation of COHbS crystals and aggregates in L-L phase separation (50 mM HEPES at pH 6.35, 1.0 g/dl COHbS, 4:1 IHP:Hb, and 10% PEG 4000, at 20°C). (*A*) Spherulite domains by ~2 min; (*B*) needle crystals and bundles of needle crystals by ~10 min; and (*C*) macrofibers and macroarrays by ~10 min. At 4000× magnification. (See Materials and Methods for explanation.)

effectively induces intermolecular attraction when the protein molecules are relatively large (Tanaka and Ataka, 2002). The role of PEG can be well interpreted by the ''depletion model,'' wherein PEG induces a ''depletion attraction'' due to an unbalanced osmotic pressure arising from the exclusion of PEG from a region between the protein particles (Asakura and Oosawa, 1958; Tardieu et al., 2002). As a result, a net attractive potential is set up by the introduction of polymer (PEG) into the solution. The preferential exclusion of PEG from proteins is due principally to the steric exclusion of PEG from the protein domain, although favorable interactions with protein surface residues, in particular nonpolar ones, may compete with the exclusion (Arakawa and Timasheff, 1985; Bhat and Timasheff, 1992).

Consistent with the depletion model, dextran (a polymer with an excluded volume effect) also induces L-L phase separation in COHb in this study. However, a higher dextran concentration (>18%, MW 67,300) is required for phase

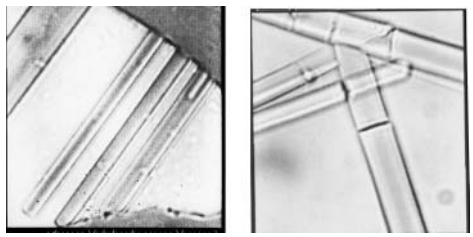

FIGURE 8 After L-L phase separation, COHbA forms orthorhombic crystals at higher Hb concentration and requires a significantly longer incubation time (>22 h). (50 mM HEPES at pH 6.35, 3.0 g/dl COHbA, 4:1 IHP:Hb, and 10% PEG 4000, at 20°C.)

separation. Furthermore, no crystals form in the same time frame as in the presence of PEG.

Participation of both PEG and IHP under low pH and low ionic strength conditions provides a unique condition for comparing solution aggregation behaviors of liganded HbA and the β6 mutant hemoglobins. The higher $T_{L\text{-}L}$ (the T^{crit} for HbC is 35°C) for the binodal curve of liganded HbC compared to HbA and HbS (Fig. 3) may be understood as follows. Hemoglobin molecules in solution interact through weak interaction forces, including electrostatic and van der Waals forces, hydrogen bonding, hydration, and hydrophobic contributions. The attractive potential of the interaction includes either van der Waals forces or the depletion components brought about by the addition of polymers such as PEG (Finet and Tardieu, 2001). Since $T_{L\text{-}L}$ has been used as a measure of the net attractive interaction, a stronger attractive hemoglobin-hemoglobin interaction in HbC is indicated. According to previous theories and simulations (Lomakin et al., 1996), the range of protein-protein interaction determines the shape and location of the phase boundaries. As the range of interaction decreases, the width of the binodal (coexistence) curve increases, and C^{crit} shifts to higher values. Therefore, since the lowest C^{crit} is observed for COHbC (Fig. 3), we conclude that COHbC has the longest interaction range among the three hemoglobins.

It is noteworthy that the L-L phase boundary varies with the concentration of IHP and PEG (Fig. 4). This could be understood in that IHP and PEG altered the Hb intermolecular interaction. The PEG-induced depletion attraction strengthens with increasing concentration of PEG (Fig. 4 *B*). In addition to the depletion attraction, PEG also causes conformational changes in Hb and thereby alters the intermolecular interactions. This is supported by the report that lower molecular weight PEG (PEG 200 at a concentration of 30%) shifted the $R \leftrightarrow T$ equilibrium in favor of low affinity T-state at pH 7.3 phosphate buffer (Goldbeck et al., 2001).

The differential modulations of the phase diagrams by the allosteric effector IHP provide direct evidence that its effects are not charge-related. The increased $T_{L\text{-}L}$ (with a corresponding lower Hb concentration) correlated with increasing IHP:Hb mole ratio (Fig. 4 *A*), indicating increased attraction between the Hb molecules. The enhanced attraction can be explained by a conformational change—it is well established that IHP binds specifically to Hb, inducing a conformational alteration. This conclusion is consistent with our earlier findings that IHP enhances liganded HbC nucleation in concentrated phosphate buffer, conditions that negate electrostatic influence (Hirsch et al., 1997). A likely mechanism is that the conformational change exposes additional hydrophobic parts of Hb molecules. Thus, it appears that hydrophobicity and the related water structuring may be the primary driving forces of the enhanced molecular interaction of liganded HbC > HbS > HbA. This conclusion is consistent with our recent findings that the crystallization of liganded HbC is entropically driven, with the loss of 10 water molecules for each tetramer contact interaction (Vekilov et al., 2002).

Control studies with chloride lend further support that IHP acts via a conformational effect rather than by a charge effect to induce L-L phase separation. No phase separation occurred when IHP was replaced with another anion such as chloride or nitrate. In the presence of IHP, the addition of chloride diminishes the IHP-induced L-L phase separation, shifting the binodal curves to the right, and concomitantly decreasing $T_{L\text{-}L}$, indicating increased repulsion between the Hb molecules (Fig. 5). This is opposite to the effect observed with increasing IHP concentrations that results in increased intermolecular attraction (i.e., increased $T_{L\text{-}L}$; see Fig. 4 *A*). Moreover, higher salt concentrations lead to enhanced charge screening. Thus, coupled with the low pH crystal structure of COHbA (Safo et al., 2002), the overall evidence is in support of a conformationally driven IHP effect, and the insignificance of the charge effect of IHP, in inducing L-L phase separation. In conclusion, the absolute differences of $T_{L\text{-}L}$ for the different hemoglobins in the presence of IHP and chloride are consistent with HbC exhibiting the strongest intermolecular attraction.

Since the surrounding water mediates the interaction of proteins, the asymmetric binodal curve of HbC may be explained in terms of a temperature-dependent depth of the attractive well. In addition, the asymmetric curve may result from the anisotropic character of the interaction energy, where the interaction between proteins depends on their relative orientation. The extra charge distribution on the surface of HbC (β6 Lys) provides not only the net charge, but more importantly, dipole, quadrupole, and higher moments which influence the protein orientation and interaction. Furthermore, the effect of the positive charge localized in the β6 Lys residue in HbC may be related to long-range conformational fluctuations, which are likely to affect the nature of interaction, making its liganded aggregation properties distinct from the HbA and HbS (Hirsch et al., 1996, 1999).

L-L phase separation and subsequent nucleation

In general, phase separation is not required for crystal growth, but in some cases, there is an intimate relationship between crystal growth and the high protein concentration liquid phase (McPherson, 1985; Ray and Bracer, 1986; Kuznetsov et al., 1999, 2001). Since nucleation of protein crystals is enhanced in the proximity of the L-L phase separation, the phase boundary is thought to be implicated in protein crystallization kinetics (Muschol and Rosenberger, 1997; ten Wolde and Frenkel, 1997; Galkin and Vekilov, 2000; Serrano et al., 2001; Galkin et al., 2002; Tanaka and Ataka, 2002). It has recently been shown for lysozyme that the process of phase separation in solution affects the kinetics of nucleation of protein crystals and that the nucleation rate can be controlled by shifting the L-L phase

boundary (Galkin and Vekilov, 2000). The above sets the theoretical basis to compare L-L phase separation and subsequent aggregation events of COHbC, COHbS, and COHbA. Under the conditions investigated, the significance of this model is demonstrated by the formation of crystals and fibers (unique to the specific hemoglobin) from L-L phase separation in the liganded β6 mutants (but not for HbA) in the same time frame (Figs. 6–8).

In addition to the R-state tetragonal crystal, a T-like aggregation style is seen for COHbC (Fig. 6) with a representative formation of flat hexagonal crystals (Hirsch et al., 2001). The T-like quaternary conformation may be induced by the conditions of this study (low pH, the presence of IHP, and PEG 4000). This possibility is supported by the low pH liganded crystal structure proposed as an intermediate structure between R and T (Safo et al., 2002), which would also explain why the fascicles of macrofibers seen for COHbS (Fig. 7 *C*) are similar to deoxy HbS macrofibers formed in acidic PEG (Vassar et al., 1982). At low pH, deoxy HbS macrofiber formation is a prelude to crystal formation, similar to that reported for oxy and deoxy HbC at neutral pH under conditions of concentrated phosphate buffer (Hirsch et al., 2001).

Needle-like crystals of COHbS appear as gel-like aggregates at high temperatures (>55°C) when viewed under the video-enhanced DIC microscope. This behavior of COHbS at high temperature is reminiscent of deoxy HbS needle crystals that formed from gently stirred solutions, which gelled upon raising the temperature (Pumphrey and Steinhardt, 1976, 1977; Jones and Steinhardt, 1979). The composite of R- and T-like solution aggregation behavior indicates that this is a conformation-driven event.

The growth of these Hb crystals after liquid-liquid phase separation may be explained in terms of thermodynamics. For HbA, crystals were formed after a significantly extended time period (Fig. 8), but only under conditions approaching the critical point for the L-L phase separation (T^{crit}, C^{crit}) (Fig. 4 *A* and Fig. 8). This behavior of HbA may be elucidated by recent theoretical studies predicting that as the system approaches the critical point for the L-L phase separation (T^{crit}, C^{crit}), the nucleation barrier ΔG is reduced, and the rate of crystal nucleation is enhanced (Galkin and Vekilov, 2000). In contrast, solutions of liganded HbC and HbS that eventually gave rise to crystals were not at the critical condition of the L-L phase diagram. Thus, the interfaces of the dense protein phase or aggregate appear to serve as nucleation sites for crystal formation (Fig. 6).

The growth of HbC crystals at the surface of the liquid-liquid interface (Fig. 6), although striking, is not surprising. Such edge effects on crystal growth have been reported before: the high protein concentration phase may create an interface between the two phases that serves as a nucleation center for crystal growth (McPherson, 1985; Ray and Bracer, 1986; Kuznetsov et al., 1999, 2001). Crystals were observed to nucleate on the surfaces of dense protein liquid droplets, always growing outward into the exterior (toward low concentration) (Kuznetsov et al., 2001). Furthermore, interfaces have been useful in generating thin, flat crystals of biological macromolecules for electron microscopy and crystallographic applications (e.g., Glaeser et al., 1991; Auer et al., 1999; Lenne et al., 2000). It has long been known that protein solutions increase their concentration as they approach an interface (MacRitchie and Alexander, 1963). This subject has been visited recently using infrared reflection absorption spectroscopy in a solution of β-casein (Meinders et al., 2001). The authors find that in a thin interface layer, the protein concentration was 15–2500 times higher than the subphase depending on the initial concentration. Another aspect of the same issue is the rapid diffusion of molecules observed at L-L interfaces that can accelerate nucleation (Lin et al., 2003).

CONCLUSION

Under the conditions employed, L-L phase separation of liganded HbC, HbS, and HbA is an event influenced by the quaternary structure and serves to amplify the microscopic intermolecular interaction differences among these Hb variants. It is demonstrated that liganded HbC exhibits 1), a stronger net attractive intermolecular interaction than liganded HbA and HbS and 2), a longer range of intermolecular interaction than HbA and HbS. Liganded HbC nucleation and crystallization may be regulated in the early stage of L-L phase separation by allosteric effectors. The L-L phase separation droplet interface participates in nucleation. Given the above differences in L-L phase separation of liganded HbC, HbS, and HbA, dynamic quaternary structural differences in these variants are implied compared to each other and to HbA. Furthermore, liganded HbS may give rise to L-L phase separation through different molecular mechanisms than deoxy HbS, consistent with their variation in structural properties (e.g., polymerization versus mechanical instability). This conclusion is consistent with the model that different pathways to the formation of higher-ordered aggregates exist for these β6 mutant hemoglobins (Hirsch et al., 2001). The combined results indicate that specific contact sites, thermodynamics, and kinetics all play a role in L-L phase separation and differ for β6 mutant hemoglobins compared to HbA.

This work was supported in part by the American Heart Association (Grant-in-Aid No. 0256390T); the National Aeronautics and Space Administration (NAG8-1824 and NAG8-1854); and the National Institutes of Health (HL 70994; RR 12248; NIH R01 HL 58247; NIH R01 HL 58038; NIH P01 38655; and NIH P01 HL 55435).

REFERENCES

Amiconi, G., and B. Giardina. 1981. Measurement of binding of nonheme ligands to hemoglobins. *Methods Enzymol.* 76:533–552.

Annunziata, O., N. Asherie, A. Lomakin, J. Pande, O. Ogun, and G. B. Benedek. 2002. Effect of polyethylene glycol on the liquid-liquid phase transition in aqueous protein solutions. *Proc. Natl. Acad. Sci. USA.* 99:14165–14170.

Annunziata, O., O. Ogun, and G. B. Benedek. 2003. Observation of liquid-liquid phase separation for eye lens γS-crystallin. *Proc. Natl. Acad. Sci. USA.* 100:970–974.

Antonini, E., and M. Brunori. 1971. Hemoglobin and Myoglobin in Their Reactions with Ligands. North-Holland, Amsterdam, The Netherlands. 110–112.

Arakawa, T., and S. N. Timasheff. 1985. Mechanism of poly(ethylene glycol) interaction with proteins. *Biochemistry.* 24:6756–6762.

Asakura, S., and F. Oosawa. 1958. Interaction between particles suspended in solutions of macromolecules. *J. Poly. Sci.* 33:183–192.

Auer, M., G. A. Scarbourough, and W. Kuhlbrandt. 1999. Surface crystallization of the plasma membrane H^+-ATPase on a carbon support film for electron crystallography. *J. Mol. Biol.* 287:961–968.

Benedek, G. B., J. Pande, G. M. Thurston, and J. I. Clark. 1999. Theoretical and experimental basis for the inhibition of cataract. *Prog. Retin. Eye Res.* 18:391–402.

Bhat, R., and S. N. Timasheff. 1992. Steric exclusion is the principal source of the preferential hydration of proteins in the presence of polyethylene glycols. *Protein Sci.* 1:1133–1143.

Broide, M. L., C. R. Berland, J. Pande, O. Ogun, and G. B. Benedek. 1991. Binary-liquid phase separation of lens protein solutions. *Proc. Natl. Acad. Sci. USA.* 88:5660–5664.

Cahn, J. W., and J. E. Hilliard. 1958. Free energy of a nonuniform system. I. Interfacial free energy. *J. Chem. Phys.* 28:258–267.

Chuang, J. Z., H. Zhou, M. Zhu, S. H. Li, X. J. Li, and C. H. Sung. 2002. Characterization of a brain-enriched chaperone, MRJ, that inhibits Huntington aggregation and toxicity independently. *J. Biol. Chem.* 277:19831–19838.

Crowther, D. C. 2002. Familial conformational diseases and dementias. *Hum. Mutat.* 20:1–14.

Dumery, L., F. Bourdel, Y. Soussan, A. Fialkowsky, S. Viale, P. Nicolas, and M. Reboud-Ravaux. 2001. β-Amyloid protein aggregation: its implication in the physiopathology of Alzheimer's disease. *Pathol. Biol. (Paris).* 49:72–85.

Durbin, S. D., and G. Feher. 1996. Protein crystallization. *Annu. Rev. Phys. Chem.* 47:171–204.

Eaton, W. A., and J. Hofrichter. 1990. Sickle cell hemoglobin polymerization. *Adv. Protein Chem.* 40:263–279.

Finet, S., and A. Tardieu. 2001. α-crystallin interaction forces studied by small angle x-ray scattering and numerical simulations. *J Cryst. Growth.* 232:40–49.

Galkin, O., and P. G. Vekilov. 2000. Control of protein crystal nucleation around the metastable liquid-liquid phase boundary. *Proc. Natl. Acad. Sci. USA.* 97:6277–6281.

Galkin, O., K. Chen, R. L. Nagel, R. E. Hirsch, and P. G. Vekilov. 2002. Liquid-liquid separation in solutions of normal and sickle cell hemoglobin. *Proc. Natl. Acad. Sci. USA.* 99:8479–8483.

Glaeser, R. M., A. Zilker, M. Radermacher, H. E. Gaub, T. Hartment, and W. Baumeister. 1991. Interfacial energies and surface tension forces involved in the preparation of thin, flat crystals of biological macromolecules for high-resolution electron microscopy. *J. Microsc.* 161: 21–45.

Goldbeck, R. A., S. J. Paquette, and D. S. Kliger. 2001. The effect of water on the rate of conformational change in protein allostery. *Biophys. J.* 81:2919–2934.

Gottfried, D. S., L. J. Juszczak, N. A. Fataliev, A. S. Acharya, R. E. Hirsch, and J. M. Friedman. 1997. Probing the hemoglobin central cavity by direct quantification of effector binding using fluorescence lifetime methods. *J. Biol. Chem.* 272:1571–1578.

Grigsby, J. J., H. W. Blanch, and J. M. Prausnitz. 2001. Cloud-point temperatures for lysozyme in electrolyte solutions: effect of salt type, salt concentration and pH. *Biophys. Chem.* 91:231–243.

Hagen, M. H. J., and D. Frenkel. 1994. Determination of phase diagram for the hard-core attractive Yukawa system. *J. Chem. Phys.* 101:4093–4097.

Herskovits, T. T., S. M. Cavanagh, and R. C. San George. 1977. Light-scattering investigations of the subunit dissociation of human hemoglobin A. Effects of various neutral salts. *Biochemistry.* 16:5795–5801.

Hirsch, R. E., C. Raventos-Suarez, J. A. Olson, and R. L. Nagel. 1985. Ligand state of intraerythrocytic circulating HbC crystals in homozygote CC patients. *Blood.* 66:775–777.

Hirsch, R. E., M. J. Lin, G. J. Vidugirus, S. Huang, J. M. Friedman, R. L. Nagel, and G. V. Vidugirus. 1996. Conformational changes in oxyhemoglobin C (β6 Glu → Lys) detected by spectroscopic probing. *J. Biol. Chem.* 271:372–375.

Hirsch, R. E., A. C. Rybicki, N. A. Fataliev, M. J. Lin, J. M. Friedman, and R. L. Nagel. 1997. A potential determinant of enhanced crystallization of HbC: spectroscopic and functional evidence of an alteration in the central cavity of oxyHbC. *Br. J. Haematol.* 98:583–588.

Hirsch, R. E., L. J. Juszczak, N. A. Fataliev, J. M. Friedman, and R. L. Nagel. 1999. Solution-active structural alterations in liganded hemoglobins C (β6 Glu → Lys) and S (β6 Glu → Val). *J. Biol. Chem.* 274:13777–13782.

Hirsch, R. E., R. E. Samuel, N. A. Fataliev, M. J. Pollack, O. Galkin, P. G. Vekilov, and R. L. Nagel. 2001. Differential pathways in oxy and deoxy HbC aggregation/crystallization. *Proteins.* 42:99–107.

Imai, K. 1982. Allosteric Effects in Hemoglobin. Cambridge University Press, NY.

Jones, M. M., and J. Steinhardt. 1979. Thermodynamic study of the crystallization of sickle-cell deoxyhemoglobin (hemoglobin S solubility/saturation concentration/enthalpy of crystallization/entropy of crystallization). *J. Mol. Biol.* 129:83–91.

Kuznetsov, Y. G., A. J. Malkin, and A. McPherson. 1999. AFM studies of the nucleation and growth mechanisms of macromolecular crystals. *J. Cryst. Growth.* 196:489–502.

Kuznetsov, Y. G., A. J. Malkin, and A. McPherson. 2001. The liquid protein phase in crystallization: a case study—intact immunoglobulins. *J. Cryst. Growth.* 232:30–39.

Lawrence, C., M. E. Fabry, and R. L. Nagel. 1991. The unique red cell heterogeneity of SC disease: crystal formation, dense reticulocytes, and unusual morphology. *Blood.* 78:2104–2112.

Lin, Y., H. Skaff, T. Emrick, A. D. Dinsmore, and T. P. Russell. 2003. Nanoparticle assembly and transport at liquid/liquid interfaces. *Science.* 299:226–229.

Lomakin, A., N. Asherie, and G. B. Benedek. 1996. Monte Carlo study of phase separation in aqueous protein solutions. *J. Chem. Phys.* 104: 1646–1656.

Lenne, P. F., B. Berge, A. Renault, C. Zakri, C. Venien-Bryan, S. Courty, F. Balavoine, W. Bergsma-Schutter, A. Brisson, G. Gruber, N. Boudet, O. Konovalov, and J. F. Legrand. 2000. Synchrotron radiation diffraction from two-dimensional protein crystals at the air/water interface. *Biophys. J.* 79:496–500.

MacRitchie, F., and A. E. Alexander. 1963. Kinetics of adsorption of proteins at interfaces. I. The role of bulk diffusion in adsorption. *J. Coll. Interf. Sci.* 18:453–456.

McPherson, A. 1982. Preparation and Analysis of Protein Crystals. Wiley, New York.

McPherson, A. 1985. Use of polyethylene glycol in the crystallization of macromolecules. *Methods Enzymol.* 114:120–125.

McPherson, A., Y. G. Kuznetsov, and A. J. Malkin. 2000. Investigation on nucleation of macromolecular crystals. 8th International Conference on the Crystallization of Biological Macromolecules. May 14–19, Florida.

Meinders, M. B., G. G. van der Bosch, and H. H. Jongh. 2001. Adsorption properties of proteins at and near the air/water interface from IRRAS spectra of proteins. *Eur. Biophys. J.* 30:256–267.

Muschol, M., and F. Bonnete. 1996. Model of attractive interactions to account for fluid-fluid phase separation of protein solutions. *J. Chem. Phys.* 105:3290–3330.

Muschol, M., and F. Rosenberger. 1997. Liquid-liquid phase separation in supersaturated lysozyme solutions and associated precipitate formation/crystallization. *J. Chem. Phys.* 107:1953–1962.

Nagel, R. L., and C. Lawrence. 1999. The Distinct Pathology of SC Disease: Therapeutic Implications. R. L. Nagel, editor. Hematology/Oncology Clinics of North America, W.B. Saunders Company, Philadelphia, PA. 433–451.

Nagel, R. L., and M. H. Steinberg. 2001. Disorders of Hemoglobin: Genetics, Pathophysiology, and Clinical Management. M. H. Steinberg, B. G. Forget, D. R. Higgs, and R. L. Nagel, editors. Cambridge University Press, Cambridge, UK. 711–785.

Pumphrey, J. G., and J. Steinhardt. 1976. Formation of needle-like aggregates in stirred solutions of hemoglobin S1. *Biochem. Biophys. Res. Commun.* 69:99–105.

Pumphrey, J. G., and J. Steinhardt. 1977. Crystallization of sickle hemoglobin from gently agitated solutions—an alternative to gelation. *J. Mol. Biol.* 112:359–375.

Puri, S., and K. Binder. 2001. Power laws and crossovers in off-critical surface-directed spinodal decomposition. *Phys. Rev. Lett.* 86:1797–1800.

Ray, W. J., and C. E. Bracer. 1986. Polyethylene glycol: catalytic effect on the crystallization of phosphoglucomutase at high salt concentration. *J. Cryst. Growth.* 76:562–576.

Safo, M. K., J. C. Burnett, F. N. Musayev, S. Nokuri, and D. J. Abraham. 2002. Structure of human carbonmonoxyhemoglobin at 2.16 Å: a snapshot of the allosteric transition. *Acta Crystallogr. D Biol. Crystallogr.* 58:2031–2037.

San Biagio, P. L., and M. U. Palma. 1991. Spinodal lines and Flory-Huggins free-energies for solutions of human hemoglobins HbS and HbA. *Biophys. J.* 60:508–512.

Scott, T. W., J. M. Friedman, M. Ikeda-Saito, and T. Yonetani. 1983. Subunit heterogeneity in the structure and dynamics of hemoglobin. A transient Raman study. *FEBS Lett.* 158:68–72.

Serrano, M. D., O. Galkin, S. T. Yau, B. R. Tomas, R. L. Nagel, R. E. Hirsch, and P. G. Vekilov. 2001. Are protein crystallization mechanisms relevant to understanding and control of polymerization of deoxyhemoglobin S? *J. Cryst. Growth.* 232:368–375.

Stanley, H. E. 1971. Introduction to Phase Transition and Critical Phenomena. Oxford University Press, London, UK.

Tanaka, S., and M. Ataka. 2002. Protein crystallization induced by polyethylene glycol: a model study using apoferritin. *J. Chem. Phys.* 117:3504–3510.

Tardieu, A., A. Le Verge, M. Malfois, F. Bonnete, S. Finet, M. Ries-Kautt, and L. Belloni. 1999. Protein in solution: from x-ray scattering intensities to interaction potentials. *J. Cryst. Growth.* 196:193–203.

Tardieu, A., F. Bonnete, S. Finet, and D. Vivares. 2002. Understanding salt- or PEG-induced attractive interactions to crystallize biological macromolecules. *Acta Crystal.* D58:1549–1553.

ten Wolde, P. R., and D. Frenkel. 1997. Enhancement of protein crystal nucleation by critical density fluctuations. *Science.* 277:1975–1978.

Vaiana, S. M., M. B. Palma-Vittorelli, and M. U. Palma. 2003. Time scale of protein aggregation dictated by liquid-liquid demixing. *Proteins.* 51:147–153.

Vassar, R. J., M. J. Potel, and R. Josephs. 1982. Studies of the fiber to crystal transition of sickle cell hemoglobin in acidic polyethylene glycol. *J. Mol. Biol.* 157:395–412.

Vega, L., E. de Miguel, and L. F. Rull. 1992. Phase equilibria and critical behavior of square-well fluids of variable width by Gibbs ensemble Monte Carlo simulation. *J. Chem. Phys.* 96:2296–2305.

Vekilov, P. G., A. R. Feeling-Taylor, D. N. Petsev, O. Galkin, R. L. Nagel, and R. E. Hirsch. 2002. Intermolecular interactions, nucleation, and thermodynamics of crystallization of hemoglobin C. *Biophys. J.* 83:1147–1156.